Short Papers

Voltage-Controlled Biphase Attenuator and Vector Synthesizer for Monolithic Microwave Signal Processors

Yoshinori Suzuki, Takashi Ohira, and Hiroyo Ogawa

***Abstract*— A GaAs monolithic voltage-controlled biphase attenuator and a vector synthesizer, which utilize remote-pinchoff cold field-effect transistors (RePOFET's), are newly developed for microwave signal-processor applications. Their features are very small circuit size, which permits dense integration, and high control linearity. Lumped-constant topologies and internal impedance optimization successfully reduce the sizes of the attenuator and vector synthesizer to just 0.5 and 2.1 mm^2, respectively. The control sensitivity deviation exhibited is within ±5% for over 50% of the full control range. The uniformity of the measured vector constellation is also improved by the RePOFET's.**

***Index Terms*— Attenuator, FET varistor, pinchoff, signal processing, vector synthesizer.**

I. Introduction

Microwave signal processing (MSP) is an emerging technology based on recent progress in monolithic microwave integrated circuits (MMIC's). The concept of MSP is analogous to digital signal processing (DSP), and processes analog signals directly at microwave frequencies. Since MSP is basically analog, modulated or multicarrier signals can be handled simultaneously without the need for any demultiplexers or demodulators. MSP currently offers lower processing functionality than DSP, but the gap is being narrowed due to the rapid progress of dense large-scale circuit-integration technologies. The characteristics of a "microwave signal processor" can be described as follows.

1) It consists of a few kinds of simple and small basic microwave circuit cells.
2) Organic functions are derived by cascading large numbers of these unit cells.
3) Unit cells include control elements so that functions can be changed as required.

The ultimate objective of MSP is adaptive or intelligent signal processing at microwave frequencies. When high-level MSP devices become available, they will replace the currently used RF-to-baseband converters and analog-to-digital converters in RF systems. They will be very cost- and space-effective, especially in parallel signal-flow networks such as beamformers for phased-array antennas [1]–[3]. The breakthrough in MSP development will be large-scale and dense integration in microwave circuits. Conventional MMIC's are composed of several to several tens of circuit elements. However, hundreds or even thousands of elements would be necessary for MSP implementation. The first step to achieving large-scale microwave device integration is to develop unit cells that are small and have low power consumption.

This paper presents the development of a variable attenuator and a vector synthesizer, which will be unit cells for MSP. They provide two fundamental functions: scalar and vector control of signal amplitude, respectively. Lumped-constant circuit topologies are employed and their optimum impedance is discussed for circuit area minimization. To control the signal amplitude with very low dc power dissipation, cold FET devices [4] are utilized in these unit cells. A novel device, called a remote-pinchoff cold FET (RePOFET), is proposed as a way to improve control linearity.

Manuscript received May 1, 1998; revised August 7, 1998.

The authors are with NTT Wireless Systems Laboratories, Yokosuka 2390847, Japan.

Publisher Item Identifier S 0018-9480(98)08341-0.

II. RePOFET Varistor

The varistor, i.e., variable resistor, is a basic element for amplitude control and is commonly used in variable attenuators [4] and variable-gain amplifiers [5]. For MSP realization, the cold-FET varistor is appropriate because it dissipates dc power (much less dc power) than do traditionally used p-i-n–diode varistors. The drain-to-source current I_{DS} in a normally biased FET is characterized as

$$\begin{aligned} I_{\mathrm{DS}} &= \frac{\beta}{2}\left\{2(V_{\mathrm{GS}}-V_T)V_{\mathrm{DS}}-V_{\mathrm{DS}}^2\right\}, \qquad \text{for } 0 \le V_{\mathrm{DS}} < V_{\mathrm{GS}}-V_T \\ I_{\mathrm{DS}} &= \frac{\beta}{2}(V_{\mathrm{GS}}-V_T), \qquad \text{for } V_{\mathrm{GS}}-V_T \le V_{\mathrm{DS}} \\ I_{\mathrm{DS}} &= 0, \qquad \text{for } V_{\mathrm{GS}} < V_T \end{aligned} \tag{1}$$

where V_{DS} is drain-to-source voltage, V_{GS} is gate-to-source voltage, V_T is threshold voltage, and β is the gain constant. Imposing the cold condition (i.e., drain-to-source dc voltage equals zero) upon (1) yields the following drain-to-source conductance:

$$\begin{aligned} G(V_{\mathrm{GS}}) &= \left.\frac{\partial I_{\mathrm{DS}}}{\partial V_{\mathrm{DS}}}\right|_{V_{\mathrm{DS}}=0} = \beta(V_{\mathrm{GS}}-V_T), \qquad \text{for } V_{\mathrm{GS}} > V_T \\ G(V_{\mathrm{GS}}) &\approx 0, \qquad \text{for } V_{\mathrm{GS}} \le V_T. \end{aligned} \tag{2}$$

The drain-to-source conductance of a cold FET has a ratio ($G_{\max}$: $G_{\min}$) of more than 100 and it has excellent linearity for RF signals. However, the control linearity, i.e., the G_{DS}–V_{GS} curve, is often limited due to the depletion-layer profile beneath the Schottky gate. This G_{DS}–V_{GS} nonlinearity would affect the amplitude control resolution of the system. We propose the RePOFET shown in Fig. 1. The RePOFET features interdigitated drain/source electrodes that sandwich a meander-shaped gate electrode. The gate electrode is punctuated piece-by-piece with resistors located on every turn of the meander. The gate of each FET is driven proportionally by the external dc control voltage. Therefore, the RePOFET pinches off the current more gradually than does the normal FET. The RePOFET cannot be used for signal amplification, but is advantageous in terms of amplitude control under the above-mentioned cold bias condition. In order to analyze the G_{DS}–V_{GS} characteristics of a RePOFET, we regard it as a parallel connection of unit FET's. As a function of V_{GS}, the total G_{DS} is formulated as

$$G(V) = \sum_{i=1}^{N} \alpha_i g(\gamma_i V), \qquad 0 < \gamma_1 \le \gamma_2 \le \cdots \le \gamma_i \le \cdots \le \gamma_n \le 1 \tag{3}$$

where α_i is the gatewidth of the ith piece of RePOFET, γ_i is the voltage ratio for the ith gate, and $g(V)$ is drain–source conductance per unit gate length. Gate width and voltage ratio can be optimized for individual circuit designs to achieve the required control linearity. An example of optimization is introduced in Section III.

0018–9480/98$10.00 © 1998 IEEE

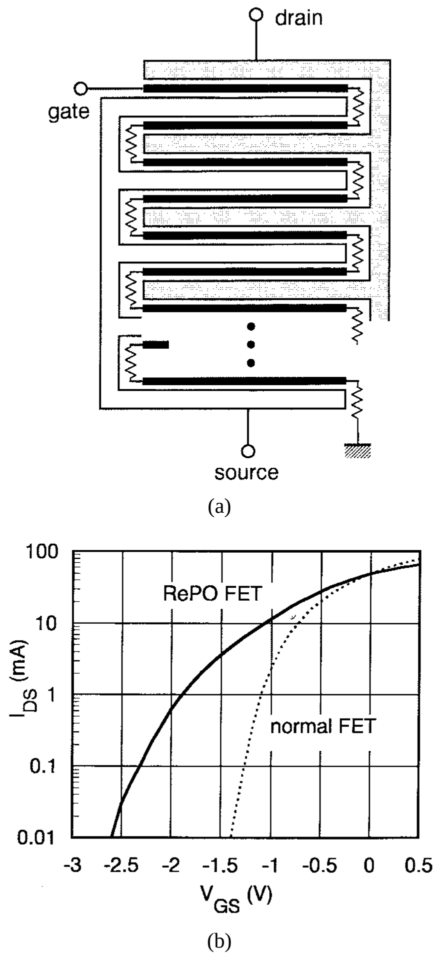

Fig. 1. RePOFET. (a) Device configuration and (b) measured $I_{\rm DS}$–$V_{\rm GS}$ characteristics for $Wg = 480\ \mu$m and $V_{\rm DS} = +3.0$ V.

III. Biphase Attenuator

We first use the RePOFET in a voltage-controlled biphase attenuator. This attenuator performs both variable attenuation and $0/\pi$ phase control. In other words, it controls both amplitude and sign, and it operates as both an inverting and noninverting variable attenuator. The voltage-controlled biphase attenuator, shown in Fig. 2(b), utilizes twin variable-resistance circuits interlocked by a single control dc line. The RF transfer function S_{21} of the circuit is given by

$$S_{21}(V) = \frac{Y_0 - G(V)}{Y_0 + G(V)} \tag{4}$$

where $G(V)$ is the variable conductance of the RePOFET, V is the control voltage, and Y_0 is the characteristic admittance of the quadrature 3-dB hybrid composed of lumped-constant inductors and capacitors. It is determined that they meet the input- and output-impedance matching requirements at the center frequency ω_0, resulting in

$$C_1 = \frac{Y_0}{\omega_0} \quad C_2 = \frac{\sqrt{2}Y_0}{\omega_0} \quad L = \frac{1}{1+\sqrt{2}}\frac{1}{\omega_0 Y_0}. \tag{5}$$

The output phase $\angle S_{21}$ is deduced from (4) as

$$\angle S_{21} = \frac{\pi}{2}, \qquad \text{for } G > Yo$$

and

$$\angle S_{21} = -\frac{\pi}{2}, \qquad \text{for } G < Yo. \tag{6}$$

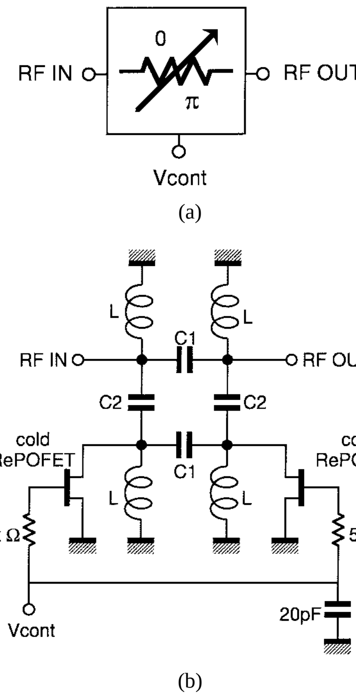

Fig. 2. Voltage-controlled biphase attenuator. (a) Symbol and (b) circuit topology.

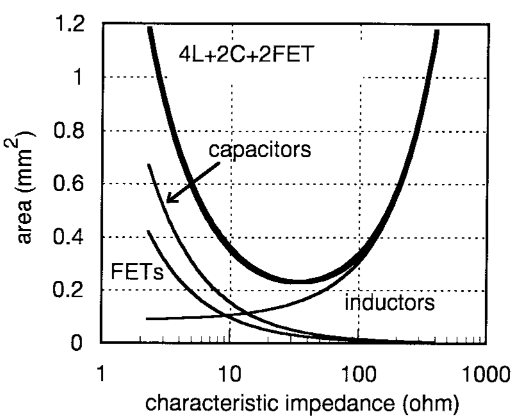

Fig. 3. Estimated circuit area for the voltage-controlled biphase attenuator, which consists of four spiral inductors, four MIM capacitors, and two FET's. Substrate $\varepsilon_r = 12.9$, inductor line/space $= 10\ \mu$m/$10\ \mu$m, MIM $C = 0.45$ pF/μm^2, $f = 2.5$ GHz.

Therefore, to achieve phase inversion, the variable conductance $G(V)$ should cover both sides of Y_0. This means $G_{\min} < Y_0 < G_{\max}$. Especially if the conductance state

$$G_{\min} \times G_{\max} = Y_0^2 \tag{7}$$

is satisfied, both phase states have equal attenuation range.

Based on this principle, a prototype voltage-controlled biphase attenuator was designed for 2.5-GHz operation and was fabricated using the GaAs MMIC process. The attenuator consists of four spiral inductors, four metal–insulator–metal (MIM) capacitors, and two FET's. The circuit area estimated to be occupied by these elements for this topology is shown in Fig. 3. We find that the circuit area needed is smallest at the characteristic impedance of about 33.3 when substrate ε_r is 12.9, the inductor number of turns is three, line/space is 10 μm/10 μm, the MIM C area is 0.5 pF/μm^2, and signal frequency is 2.5 GHz, as shown in Fig. 3. For this characteristic impedance, the lumped-element constants are deduced to be $C_1 = 1.9$ pF, $C_2 = 2.7$ pF, $L = 0.88$ nH, and the total gatewidth of each RePOFET is 480 μm.

The transfer function S_{21} of the voltage-controlled biphase attenuator is a function of the conductance G, as described in (4). The gatewidth and voltage ratio of the RePOFET used in the circuit are optimized in order to achieve high control linearity. Nonlinearity is defined as the standard deviation from the ideal $S_{21}(V)$ as follows:

$$\sigma = \sqrt{\frac{1}{V_{\max} - V_{\min}} \int_{V_{\min}}^{V_{\max}} \{S_{21}(V) - S_{21\text{ideal}}(V)\}^2 \, dV} \quad (8)$$

where $S_{21\text{ideal}}(V)$ is a completely linear function of V, i.e.,

$$S_{21\text{ideal}}(V) = S_{21}(V_{\min}) + \{S_{21}(V_{\max}) - S_{21}(V_{\min})\} \frac{V - V_{\min}}{V_{\max} - V_{\min}}. \quad (9)$$

In order to find the optimum set of $\{\gamma_1, \gamma_2, \cdots, \gamma_n\}$,

$$\frac{\partial}{\partial \gamma_i} \sigma(\gamma_1, \gamma_2, \cdots, \gamma_n) = 0, \qquad i = 1, 2, \cdots, n \quad (10)$$

are solved for $\gamma_i i = 1, 2, \cdots, n,$ resulting in $\gamma_1 = 0.50, \gamma_2 = 0.50, \gamma_3 = 0.57, \gamma_4 = 0.71, \gamma_5 = 0.86$, and $\gamma_6 = 1.00$.

The gatewidth of each FET piece is set to be $\alpha_i = 80$ μm; the number of fingers n equals six in this case. The number of fingers $n = 6$ is sufficient; no further improvement can be obtained by increasing the number of fingers to seven or more. The unit gatewidth $\alpha_i = 80$ μm is chosen to satisfy the equal-attenuation condition shown in (7).

The transfer characteristics versus control voltage of the fabricated attenuator are shown in Fig. 4(a). The control characteristics are shown in Fig. 4(b) in comparison with those of conventional cold FET's. The ordinate shows differential sensitivity, which is defined as

$$\left| \frac{\Delta S_{21}}{\Delta V} \right| = \sqrt{\left(\frac{\Delta \mathrm{Re}\{S_{21}\}}{\Delta V} \right)^2 + \left(\frac{\Delta \mathrm{Im}\{S_{21}\}}{\Delta V} \right)^2}. \quad (11)$$

Sensitivity flatness within ±5% was observed for over 50% of the full varistor control range.

IV. Vector Synthesizer

The other unit cell proposed for MSP is the voltage-controlled vector synthesizer. The function of this cell is vector or complex amplitude control, which means that this unit cell can provide arbitrary phase and amplitude. The cell described in Section III performs only scalar operations. It consists of a two-way signal divider, pair of voltage-controlled biphase attenuators, and quadrature 3-dB hybrid, as shown in Fig. 5. The complex transfer function S_{21} of the circuit is the orthogonal combination of two biphase attenuators

$$S_{21}(G_1, G_2) = \frac{1}{2} \left(\frac{Y_0 - G_1}{Y_0 + G_1} + j \frac{Y_0 - G_2}{Y_0 + G_2} \right) \quad (12)$$

where G_1 and G_2 are the conductance of the varistor used in each attenuator cell. These conductance levels are controlled by a pair of external dc voltages.

A prototype vector synthesizer was designed for 2.5-GHz operation and fabricated using a GaAs MMIC process. The circuit area is 3.5 mm × 0.6 mm. The attenuator and vector synthesizer circuit areas are smaller than any reported attenuator, vector synthesizer, or endless phase shifter, as shown in Fig. 6. The measured vector constellation of the fabricated vector synthesizer is shown in Fig. 7, along with one of a conventional cold FET for comparison. $\mathrm{Re}\{S_{21}\}$ and $\mathrm{Im}\{S_{21}\}$ are around 0.1 in these figures, which means a loss

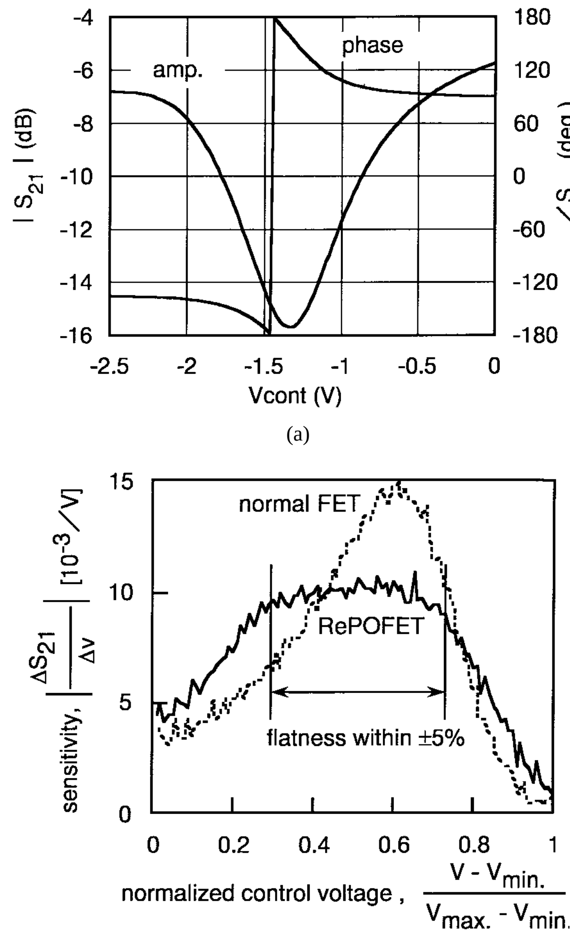

Fig. 4. Measured characteristics of the biphase attenuator. (a) S_{21} versus control voltage and (b) control voltage sensitivity. The RePOFET improves flatness of control sensitivity.

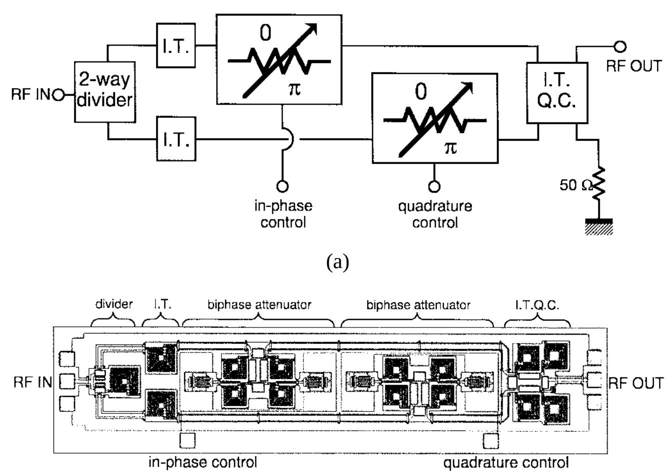

Fig. 5. Voltage-controlled vector synthesizer. (a) Block diagram and (b) prototype fabricated on GaAs substrate. It consists of a two-way power divider, pair of impedance transformers (IT's), two voltage-controlled biphase attenuators, and an impedance-transforming quadrature coupler (ITQC). The conjugate output port is terminated with an internal 50-Ω load.

of about 18 dB. It contains inherent 6-dB loss in the power divider and combiner, 2-dB excess loss in the divider, 7-dB excess loss in the attenuator, and 3-dB excess loss in the ITQC. Their

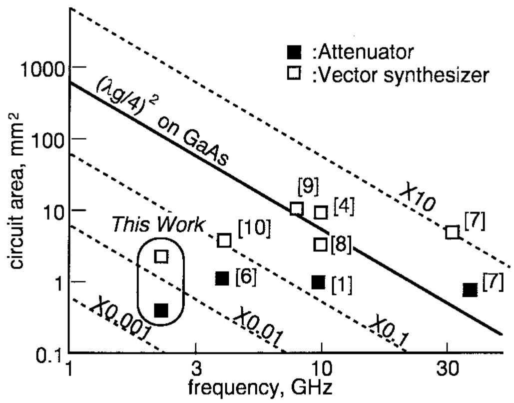

Fig. 6. Attenuator and vector synthesizer size reduction.

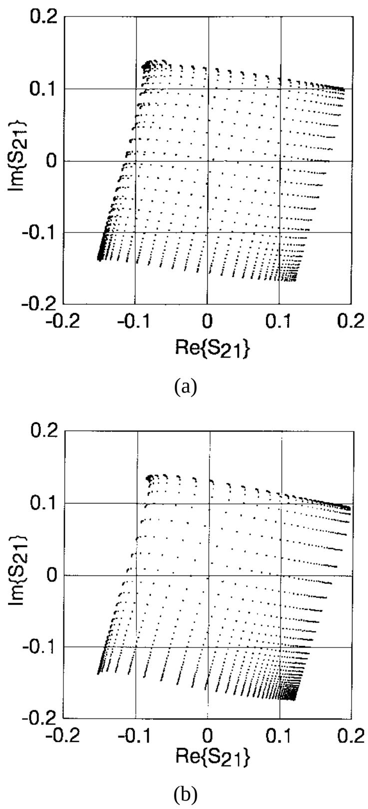

Fig. 7. Constellations generated by the vector synthesizer (a) with RePOFET's and (b) with conventional FET's. The two constellations have the same number of vector points, and the uniformity is found to be improved by the RePOFET's.

constellations were plotted by changing the in-phase and quadrature control voltages in uniform steps. The vector synthesizer using the RePOFET exhibits improved constellation uniformity. The maximum control sensitivity is improved approximately 50% from that of the conventional scheme.

V. Conclusion

The RePOFET is a powerful and flexible device for both scalar and vector amplitude control of microwave signals. Its control characteristics can be optimized for various applications. Design and optimization examples have been described in terms of control linearity. For circuit area minimization, it was shown that there exists an optimum internal impedance. By using RePOFET's and this minimization technique, a voltage-controlled biphase attenuator and vector synthesizer were designed and fabricated. These devices are remarkably small: 0.5 and 2.1 mm^2, respectively. Strong linearity improvement was also shown. The device and circuits described herein are the smallest and most power efficient to date. Although they are not yet small enough to be used in microwave signal processors, they are believed to be a major step toward realizing MSP.

Acknowledgment

The authors would like to thank H. Kamitsuna, NTT Electronics Corporation, Yokosuka, Japan, for participating in valuable discussions on GaAs MMIC design.

References

[1] S. Lucyszyn and I. D. Robertson, "Analog reflection topology building blocks for adaptive microwave signal processing applications," *IEEE Trans. Microwave Theory Tech.*, vol. 43, pp. 601–611, Mar. 1995.

[2] T. Ohira, Y. Suzuki, H. Kamitsuna, and H. Ogawa, "Megalithic microwave signal processing for phased-array beamforming and steering," *IEEE Trans. Microwave Theory Tech.*, vol. 45, pp. 2324–2332, Dec. 1997.

[3] Y. Suzuki, T. Ohira, and H. Ogawa, "A GaAs monolithic bipolar variable attenuator with improved control linearity," in *Proc. 17th AIAA Int. Commun. Satellite Syst. Conf.*, Yokohama, Japan, Feb. 1998, pp. 821–825.

[4] L. M. Devlin and B. J. Minnis, "A versatile vector modulator design for MMIC," in *IEEE MTT-S Int. Microwave Symp. Dig.*, Dallas, TX, June 1990, pp. 519–522.

[5] A. K. Ezzeddine, H. A. Hung, and H. C. Huang, "An MMAC C-band FET feedback power amplifier," *IEEE Trans. Microwave Theory Tech.*, vol. 38, pp. 350–357, Apr. 1990.

[6] D. Roques, J. L. Cazaux, and M. Pouysegur, "GaAs MMIC control functions for 3.7–4.2 GHz band active antenna," *Ann. Telecommun.*, vol. 45, no. 3/4, pp. 224–230, 1990.

[7] N. Imai and T. Imaoka, "Multilayer MMIC's and multifunctional circuits," in *IEICE MWE'96 Microwave Workshop Dig.*, Yokohama, Japan, Dec. 1996, pp. 257–262.

[8] M. Nakatsugawa and M. Muraguchi, "A monolithic endless phase shifter using quasi-transmission-line variable reactors and 3-D MMIC structure," in *Proc. 26th European Microwave Conf.*, Prague, Czech Republic, Sept. 1996, pp. 977–980.

[9] T. C. B. Tieman, A. P. de Hek, F. L. M. van den Bogaart, and W. M. A. van Hoek, "A single chip X-band phase shifter with 6 bit uncorrected phase resolution and mote than 8 bit corrected phase resolution," in *IEEE Microwave Millimeter-Wave Monolithic Circuit Symp. Dig.*, June 1992, pp. 137–140.

[10] P. Maloney, J. Selin, and G. Jones, "Continuously variable L-band monolithic phase shifters using GaAs," in *IEEE GaAs IC Symp. Dig.*, Grenelefe, FL, Oct. 1986, pp. 78–81.